Development of an Innovative Extension for Fatigue Life Monitoring Using a Piezoelectric Sensor

Ghaderiaram, Aliakbar; Mohammadi, Reza; Schlangen, Erik; Fotouhi, Mohammad

Fracture, Damage and Structural Health Monitoring

Development of an Innovative Extension for Fatigue Life Monitoring Using a Piezoelectric Sensor

Aliakbar Ghaderiaram[a,*], Reza Mohammadi[a], Erik Schlangen[a], and Mohammad Fotouhi[a]

aDelft University of Technology, Faculty of Civil Engineering, Delft, The Netherlands

Abstract

Engineering structures, such as bridges, wind turbines, airplanes, ships, buildings, and offshore platforms, often experience uncertain dynamic loadings due to environmental factors and operational conditions. The lack of knowledge about the load spectrum for these structures poses challenges in terms of design and can lead to either over-engineering or catastrophic failure. This research introduces a robust and innovative device, analogous to a "Fitbit" for structures, capable of measuring complex loading conditions throughout the structure's lifespan. The proposed approach involves developing a middleware, referred to as an "extension," which facilitates the transfer of mechanical deformation to a piezoelectric sensor. This approach overcomes challenges associated with directly attaching piezoelectric sensors to the structure's surface such as rupture possibility in higher strain and attaching on rough surfaces. The feasibility study primarily focuses on validating the performance of the extension and monitoring variation trends. The ultimate objective is to develop an Internet of Things (IoT) sensor node capable of measuring applied cyclic loads. To achieve this goal, an electronic system and embedded software will be developed to capture the complex load spectrum and convert it into a fatigue damage index for predicting the structure's fatigue life. The collected data will be transmitted to the user through a wireless communication platform. The proposed sensor design is versatile, allowing for both attachment and embedding and is demonstrated here for monitoring fatigue in engineering structures.

1. Introduction

Structural health monitoring (SHM) is essential for ensuring the safety and longevity of engineering structures. A significant demand is for durable and advanced engineering structures such as buildings, bridges, dams, tunnels, and highways. These structures are subjected to design and environmental loading conditions, and their health monitoring and maintenance are important to assure their safe operation. One critical aspect of SHM is monitoring cyclic loading and the remaining fatigue life of structures. Monitoring cyclic loadings and the remaining fatigue life of the structures is essential in health monitoring to make condition-based decisions to extend their lifetime, repair, or replace them. However, the load spectrum of most engineering structures is unknown, and there is no appropriate device to measure it, and current monitoring technologies are expensive and require significant hours of expert people and specialized equipment to assure the safe operation of the engineering structures. There have been many studies conducted on the health monitoring of engineering structures[1]–[3], and it was extended to other types of safety-critical structures. Health monitoring of concrete structures has been done using different non-destructive methods such as electromagnetic waves[4], mechanical waves[5], optical imaging[6], and optical fibers[7].

Piezoelectric sensors have emerged as a promising technology for fatigue life monitoring in engineering structures. Piezoelectric sensors work on the principle of the piezoelectric effect, which is the ability of certain materials, such as quartz, ceramics, and certain polymers, to generate an electric charge in response to mechanical stress or strain. When a piezoelectric sensor is attached to a structure, any deformation of the structure causes the sensor to generate an electric charge. This charge is then converted into a measurable signal that can be used to monitor the mechanical response of the structure[8]. These sensors can detect subtle changes in a structure's response to cyclic loading and have been used for monitoring the structural health of various materials, including metals, composites, and reinforced concrete using different methods such as ultrasonic wave propagation[9], acoustic emission[10], and strain measurement[11]. In SHM applications, piezoelectric sensors are typically attached to critical locations on the structure, such as joints, welds, and areas of high stress, where they can detect any changes in the mechanical response of the structure due to fatigue, corrosion, or other forms of damage. The sensors can be used to measure a wide range of parameters, including strain, displacement, and acceleration, depending on the specific application. Piezoelectric sensors are also highly sensitive, which makes them well-suited for detecting small changes in the structure's mechanical response that may be indicative of early-stage damage. This early detection allows for timely intervention, reducing the risk of catastrophic failure and extending the life of the structure.

To address the limitations of traditional monitoring methods, there has been growing interest in developing wireless sensor nodes for real-time monitoring of engineering structures [12]. Wireless sensor nodes can be attached or embedded in a structure, allowing for remote data collection and analysis. Overall, piezoelectric sensors are an important technology for SHM, providing a sensitive and reliable method for monitoring the health of engineering structures. When combined with wireless sensor nodes, piezoelectric sensors can provide real-time monitoring data that can be used to make informed decisions about the maintenance and repair of structures, ultimately improving their safety and longevity[13].

This research project aims to develop an innovative wireless fatigue life monitoring system utilizing piezoelectric sensors. The system can be conveniently attached or embedded into various engineering structures, with a particular emphasis on civil engineering materials like metals and reinforced concretes, as well as applications such as bridges. The primary objective is to employ piezoelectric sensors as strain gauges; however, there are challenges associated with this approach, including the limited range of strain to failure of PZT sensors and the issue of directly attaching them to high-strain structures. To overcome these challenges, inspiration was drawn from a previous study on impedance measurement [14] utilizing piezoelectric technology. Consequently, a novel approach has been introduced in the form of a middleware or "extension" to address the strain limitation issue. This method involves converting one-dimensional strain into bending and subsequently leveraging the two distinct strain-charge coefficients of the piezoelectric sensors.

The paper will describe the design of the fatigue life monitoring sensor node, the testing and validation process, and a middle ware design that we call it extension, which make it more portable and flexible to use, highlighting its potential impact on the field of structural engineering. The development of such a system is expected to revolutionize fatigue life monitoring, providing a low-cost, low-power, and highly reliable solution for monitoring engineering structures. In conclusion, the fatigue life monitoring sensor node developed in this research project represents a significant advance in the field of structural health monitoring. Its innovative approach to detecting potential fatigue failure using piezoelectric sensors and extension combined with the flexibility and convenience of wireless technology, makes it a valuable tool for ensuring the safety and reliability of engineering structures.

2. Methodology

2.1 Fatigue failure

All structures, including critical civil infrastructure facilities like bridges and highways, deteriorate with time due to various reasons including fatigue failure caused by repetitive traffic loads, effects of environmental conditions, and extreme events such as an earthquake. Fatigue has been determined as one of the main reasons for failure in metallic structures [15], and it is the main contributor to the degradation of other types of structures such as reinforced concretes [16]. An unlimited stress level is defined as the stress level below which no fatigue failure

occurs in some materials such as steel, while other materials such as aluminum do not have an unlimited stress level. In cyclic loading with each stress in a range greater than infinite loading level, micro-cracks occur on the surface or bulk of the structure and these cracks grow as the loading continues [15]. By increasing the size of the cracks in a structure, the crack size reaches a critical size where the effective cross-sectional area (A) is reduced, and the applied stress $\sigma = F/A$ is greater than the failure strength of the material. As a result, once the cracks grow and become critical, the structure fails. In the mechanical properties of materials, the fatigue life is determined by the number of stress cycles at each level of stress, which is called the S-N curve [15]. The S-N curve concept, also called a Wöhler curve, is used to evaluate the fatigue life of structures. According to the applied stress history and S-N curve information, the amount of damage index (DI) due to cyclic loading can be determined by Eq. 1, where n_i is the number of cycles at the stress level of i, and N_i is the maximum number of cycles in the stress level of i. In theory, DI must be smaller than 1 to avoid fatigue failure, or this DI can be defined as the percentage of fatigue-induced damage. As mentioned before, and according to the S-N curve for some materials such as steel, there is an unlimited stress level below which, the applied stress does not cause any damage and fatigue failure to the structure.

$$DI = \sum \frac{n_i}{N_i} \tag{1}$$

2.2 Fatigue life measurement sensors

In order to use the S-N curve, the stress level needs to be measured. According to Hooke's law, there is a direct relationship between the strain and the stress levels in the materials. Therefore, measuring the strain level gives the stress level as long as the Young modulus of the material is known. Strain can be measured using different methods such as strain gauges, digital imaging, FBG, magnetic microwire, laser optic, capacitive, and magnetic sensors. Loading can also be measured directly using methods such as load cells and ultrasonic. These methods are active methods used for fatigue life measurements; however, they require a significant amount of power to be operational during the lifetime of the structures which may last years. For example, a civil engineering structure is usually expected to last over 25 years[17]. Therefore, this project is looking to develop a simple passive fatigue sensor based on piezoelectric materials for optimal measurement of fatigue life with minimal cost, high durability, and low power consumption. By using piezoelectric and triboelectric sensors, we can achieve passiveness, simplicity of fabrication, and no consumption of electric power. Of course, among these, piezoelectric sensors are more transparent and stable in terms of commercial use and relationships governing their performance (Eq. 2).

$$\begin{cases} \boldsymbol{S} = s\boldsymbol{T} + \delta^t \boldsymbol{E} & \Rightarrow & S_{ij} = \sum_{k,l} s_{ijkl}T_{kl} + \sum_{k} d^t_{ijk}\boldsymbol{E}_k \\ \boldsymbol{D} = \delta\boldsymbol{T} + \varepsilon\boldsymbol{E} & \Rightarrow & D_i = \sum_{j,k} d_{ijk}T_{jk} + \sum_{j} \varepsilon_{ij}\boldsymbol{E}_j \end{cases} \tag{2}$$

Where **S** is the linearized strain, s is compliance under short-circuit conditions, **T** is stress, and $\nabla.T = 0$, $\boldsymbol{S} = \frac{\nabla u + u\nabla}{2}$ where u is the displacement vector, δ is the piezoelectric tensor and the superscript t stands for its transpose. E is the electric field strength, D is the electric flux density (electric displacement), ε is the permittivity (free-body dielectric constant), and $\nabla.D = 0$, $\Delta \times E = 0$. Due to the symmetry of δ, $d^t_{ijk} = d_{kji} = d_{kij}$. In matrix form it can be written like as Eq. 3:

$$\begin{cases} \{\boldsymbol{S}\} = [s^E]\{\boldsymbol{T}\} + [d^t]\{\boldsymbol{E}\} \\ \{\boldsymbol{D}\} = [d]\{\boldsymbol{T}\} + [\varepsilon^T]\{\boldsymbol{E}\} \end{cases} \tag{3}$$

Where [d] is the matrix for the direct piezoelectric effect and $[d^t]$ is the matrix for the converse piezoelectric effect. The superscript E indicates a zero, or constant, electric field; the superscript T indicates a zero, or constant, stress field; and the superscript t stands for transposition of a matrix.

Among the piezoelectric sensors, there are two types of ceramic based like as PZT and polymer based like as PVDF, each of which is used in certain conditions according to the characteristics of the electric charge generation ratio on the type of strain or applied pressure (d_{ES})[18]. In this paper, a piezoelectric sensor (a P-876 PZT sensor from PI) was used. The sensor characteristics are presented in table 1.

Table 1. P-876 PZT sensor characteristics

Property	Qty	Unit
Dimensions	61×350.5	mm
Min. bending radius	20	mm
Electrical capacitance	90 ±20%	nF
Piezo ceramic	PIC255	
Piezoceramic height	200	μm
Piezoelectric charge coefficient	d_{31}=-210 / d_{33}=500	pC/N
Elastic compliance coefficient	S^E_{11}=15 / S^E_{33}=19	pm^2/N

3. Experimental Method

3.1 Materials

The test structure utilized a 6061-T6 aluminum specimen, which was carefully shaped into a dog-bone configuration to ensure effective management and control of the applied strain during the loading process. Tensile loading was applied using an Instron 8872 test machine, which had a maximum capacity of 10 kN. To obtain the stress-strain curve for the aluminum specimen, the dog-bone shape was designed to fail at approximately 7.5 kN, as depicted in Fig. 1(a). Additionally, another set of dimensions was used to have a stiffer specimens for the purpose of applying cyclic tensile loads shown in Fig. 1(b). Complete details regarding the dimensions of the specimens can be found in Table 2.
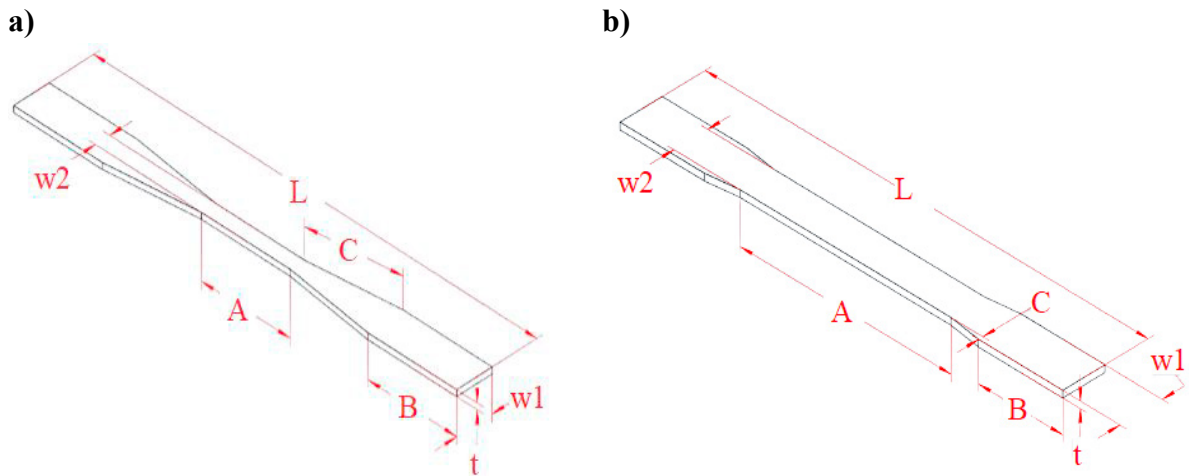

Fig. 1. The test specimen, a) specimen for yield test, and b) specimen for fatigue test

Based on the known yield stress (σ_n) and strain (ε_n) values of approximately 309 MPa and 0.5% respectively for 6061-T6 aluminum [19], calculations were performed to determine the corresponding yield force and displacement (δx) along the gauge length (A).

Table 2. Mechanical dimensions of aluminium test specimens (the manufactured specimens had ±0.1 mm tolerance due to cutting process)

Dimensions (mm)	Static failure specimen	Fatigue specimen
L	250	210
w1	20	20
w2	8	16
A	50	100
B	50	40
C	50	2
t	3	3

The results of these calculations are presented in Table 3. It can be observed that the applied tensile force of 7.5 kN corresponds to approximately 50% of the yield point in the fatigue specimen. Therefore, it is evident that a significant number of cycles would be required for the specimen to reach the failure point.

Table 3. Mechanical loading and dimensional changing parameters

Parameters	Yield specimen	Fatigue specimen
Cross-section area (t*w2)(mm2)	24.3	48.5
T_{max} (N)	7508.7	14989.5
δx along the gauge length (mm) (@ 7.5 kN)	0.22	

3.2 Test method

The purpose of incorporating an extension is to offer a user-friendly interface or plug-in that can be conveniently installed on both concrete and metallic structures. The extension, depicted in Fig. 2, is constructed using a 3D printed tough PLA material and offers the flexibility of either surface-mounting it onto the host structure or embedding it within the concrete. The piezoelectric sensor is affixed to the flexible plate, functioning as the sensor bed. One of the key advantages is the simplification of monitoring movements within the host structure, as the mechanical and electrical behaviour of the extension is well understood. This eliminates the requirement for different sensor attachments and distinct signal analysis processes for each host structure. Such variations in surface smoothness and patterns can pose challenges in traditional approaches, making the use of the extension a more efficient and reliable solution.

However, it is important to consider that direct attaching of the low strain to failure PZT sensor to a surface that has a high applied strain ranges than the sensor's strain to failure carries the risk of sensor rupture under high strains. According to the sensor datasheet[20], lateral strain is 650μm/m that is lower than aluminum substrate strain to failure. To mitigate this risk, the current design incorporates an initial bending to prevent sensor rupture during high strain levels in the host structures. The working principle of the extension is as follows: the extension legs are initially installed at a predetermined distance on the structure. Considering that the sensor length is 61 mm and the minimum bending diameter is 40 mm, the minimum distance between the extension legs should be approximately 40 mm. This allows for a 20 mm range of stretching between the legs, equivalent to a maximum bearable strain of 30%. After the installation of the extension legs, the sensor bed with the attached sensor is placed into the designated slots. As the strain varies in the host structure, this displacement is transferred to the sensor by modifying the bending diameter, resulting in the generation of an electrical signal. Additionally, Fig. 2 showcases two holders specifically designed for securing the LVDTs during tensile tests. These holders ensure the proper positioning and stability of the LVDTs throughout the testing process.
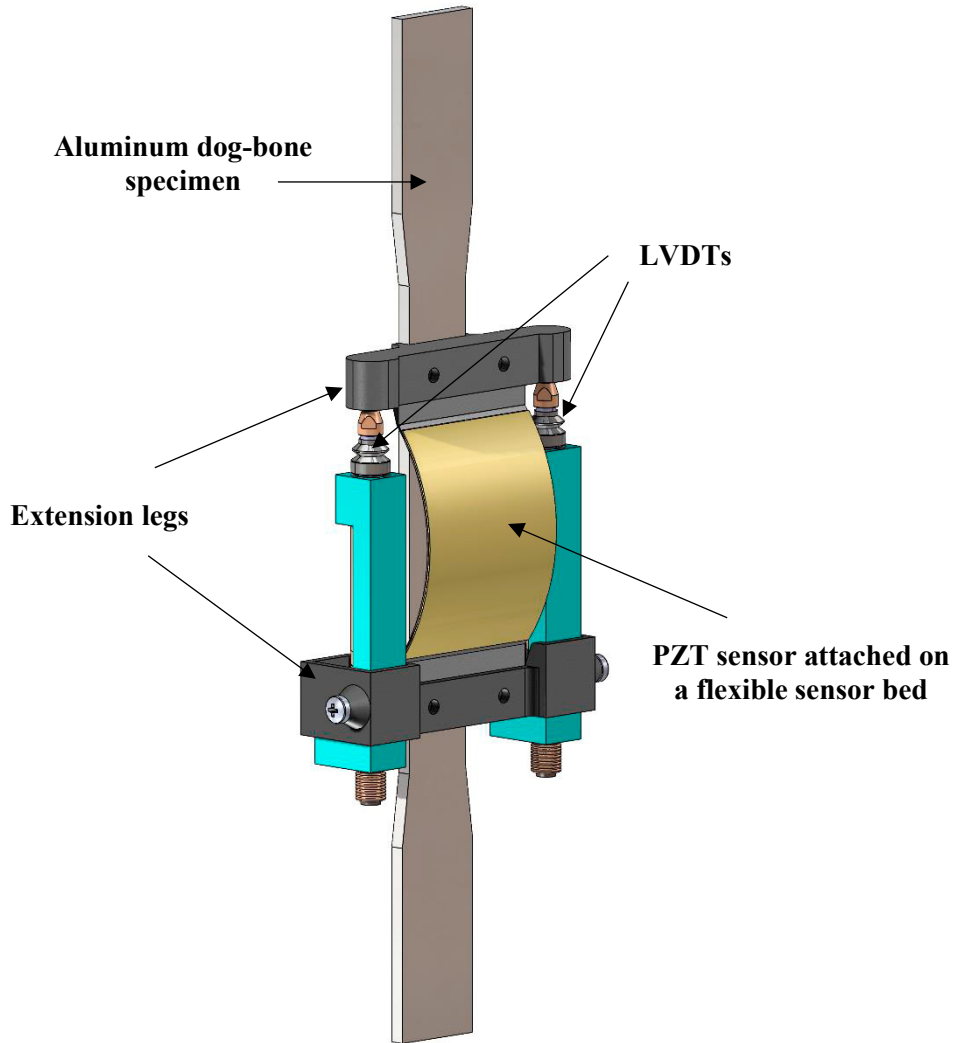
Fig. 2. Cyclic loading test setup on the dog-bone aluminum specimen containing LVDTs

4. Result and discussion

4.1. Quasi-static test

Firstly, the aluminum specimen was tested to obtain the stress-strain curve. Subsequently, the fatigue loading range was determined within the predominantly linearly elastic region. To accomplish this, three dog-bone shaped specimens were subjected to pure tensile load (Fig. 1(a)). The tension speed was set at 30 µm/sec, and the load limit was 9 kN. The results are following the calculation in table 3, and Fig. 3 illustrates the yield stress, which is approximately 293 MPa (equivalent to 7.2 kN due to a ±0.1 mm cutting error in the manufactured dimensions). S1, S2, and S3 correspond to specimens 1, 2, and 3, respectively. Additionally, Fig. 4 presents a comparison of the length variation of the test structure and specimens from their initial states.
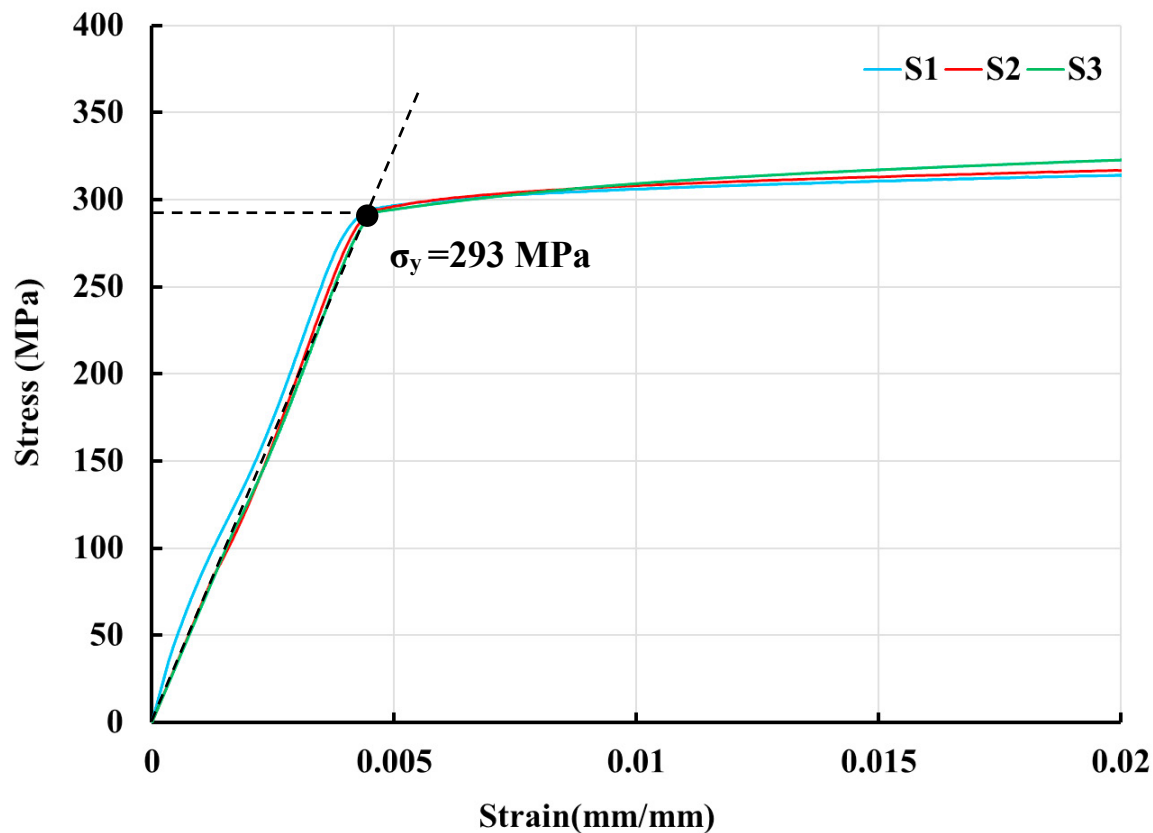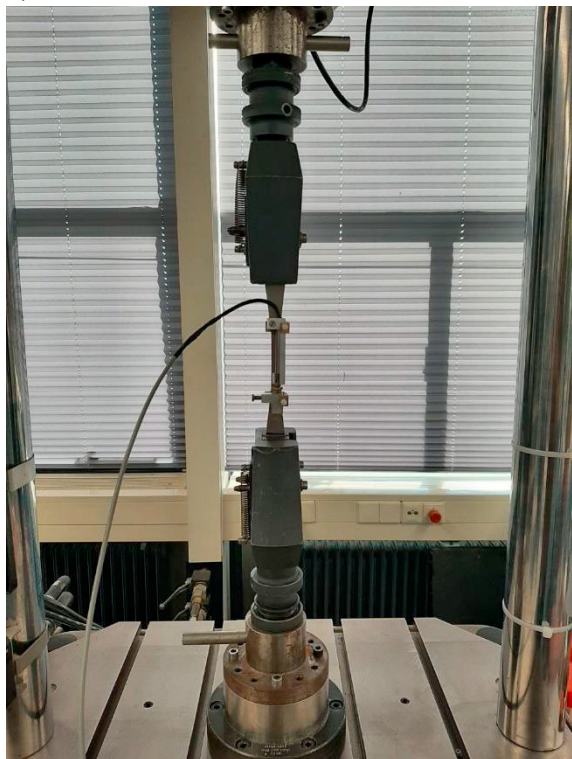
Fig. 3.Tensile stress-strain graphs for the aluminum specimens (S1~3)

Fig. 4. Yield test structure a) applying tension to a dog-bone aluminum using Instron machine and attached LVDT to measure the strain. B) Comparing two broken specimens with a true specimen

4.2. Fatigue test

The primary objective of this section was to evaluate the extension and calibrate the sensors. To achieve this, the extension was attached to the stress concentration area of the fatigue test specimen using an epoxy glue. The highest tensile load applied in this test was 8 kN, resulting in a strain of 0.23% or a displacement of 144 μm in terms of extension length. To ensure an adequate range for detecting the longest displacement, a bending diameter of 2 mm was chosen. Fig. 5 illustrates the placement of two LVDTs to measure the real strain between the extension legs.

Cyclic loads were defined between the minimum and maximum tensile points, as depicted in Fig. 6, and various loading frequencies were employed, as listed in Table 4. It is expected that, with the same cyclic loading profile, the strain applied to the specimen would remain consistent. Consequently, this strain leads to cyclic displacement between the extension legs, which is reflected in the sensor output voltage.

According to the governing equations of piezoelectric materials (Eq. 3), a higher strain generates a higher voltage, as observed in the sensor output curves in Fig. 7. Another influential parameter affecting the sensor output is the loading frequency. Since piezoelectric sensors are sensitive to dynamic excitation, higher excitations result in higher voltages. Fig. 8 demonstrates the effect of frequency variation on the sensor output. It is evident that the strain-voltage linear curves shift upward as the loading frequency increases, and there is also a slight increase in the slope of the curves at higher frequencies.

Table 4. Cyclic loading characteristic

Tensile load characteristics	Qty	Unit
Minimum	0.2	kN
Maximum	2, 4, 6, 8	kN
Frequency (sine wave)	1, 2.5, 5, 7.5, 10	Hz

The observed linear relationship between strain and voltage in the sensor output confirms the potential use of the sensor for strain monitoring. However, it is evident that the relationship is influenced by the frequency of the load. This frequency dependency highlights the need for further study and validation to establish the precise relationship between the sensor output and dynamic loading conditions. To achieve a comprehensive understanding of the sensor's response to various loading scenarios, additional investigations and validations are required. This may involve conducting controlled experiments with different loading frequencies and magnitudes to gather more data points and explain the observed trends with analytical solutions of finite element models. Once the strain-voltage relationship is thoroughly understood and validated, the next step would involve utilizing this information to calculate a reliable damage index. The damage index calculation can provide insights into the level of fatigue and potential structural deterioration based on the sensor output. This would allow for accurate predictions of the remaining fatigue life of the host structure.

In summary, there is a need for continued study and validation to understand the relationship between sensor output and dynamic loading conditions. This will enable the calculation of a reliable damage index and facilitate further investigations for monitoring the condition and behavior of the host structure.
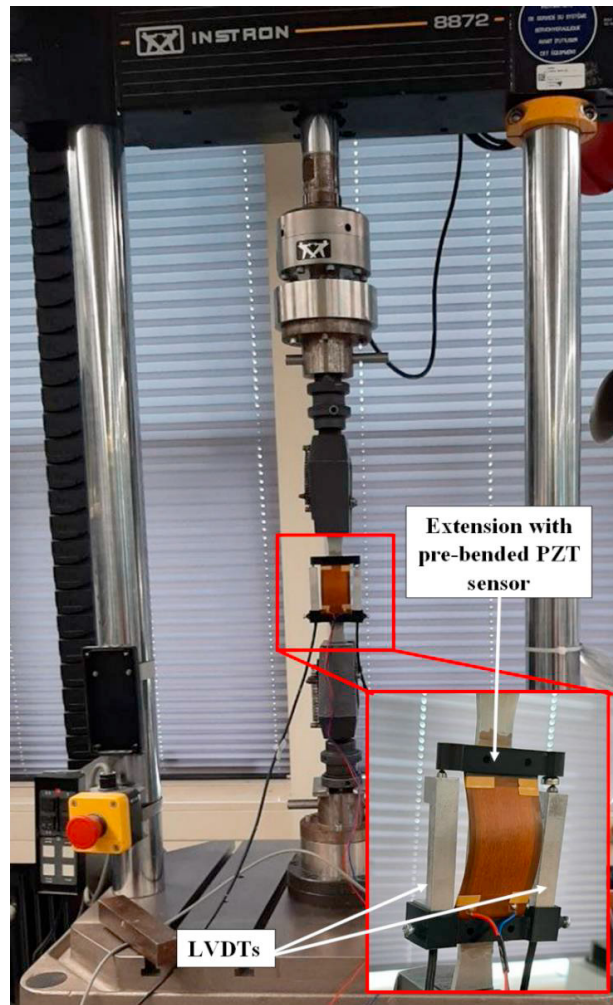
Fig. 5. Cyclic test structure using innovative extension and two LVDTs are installed on extension to get the real strain between extension legs.
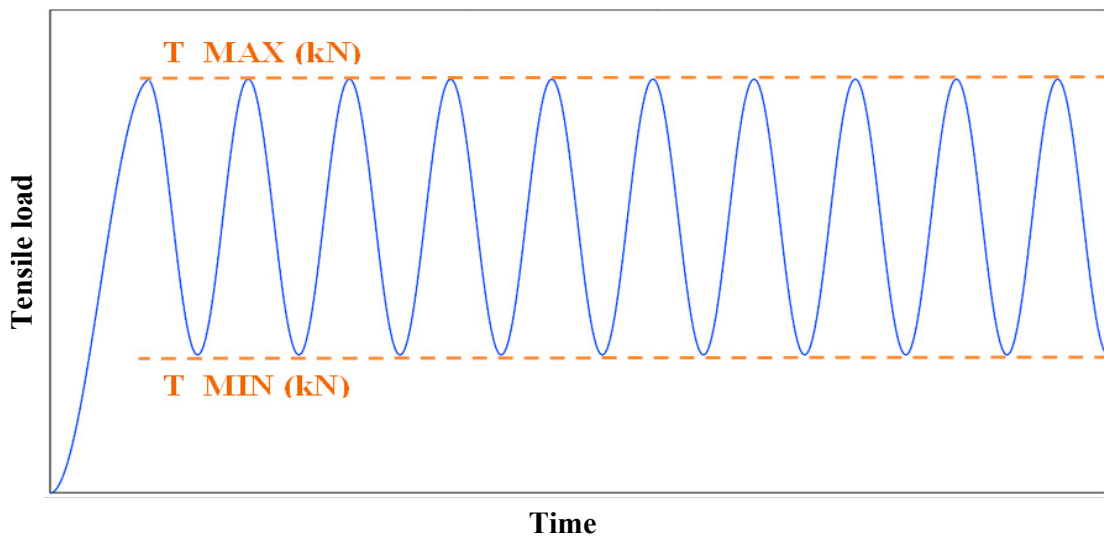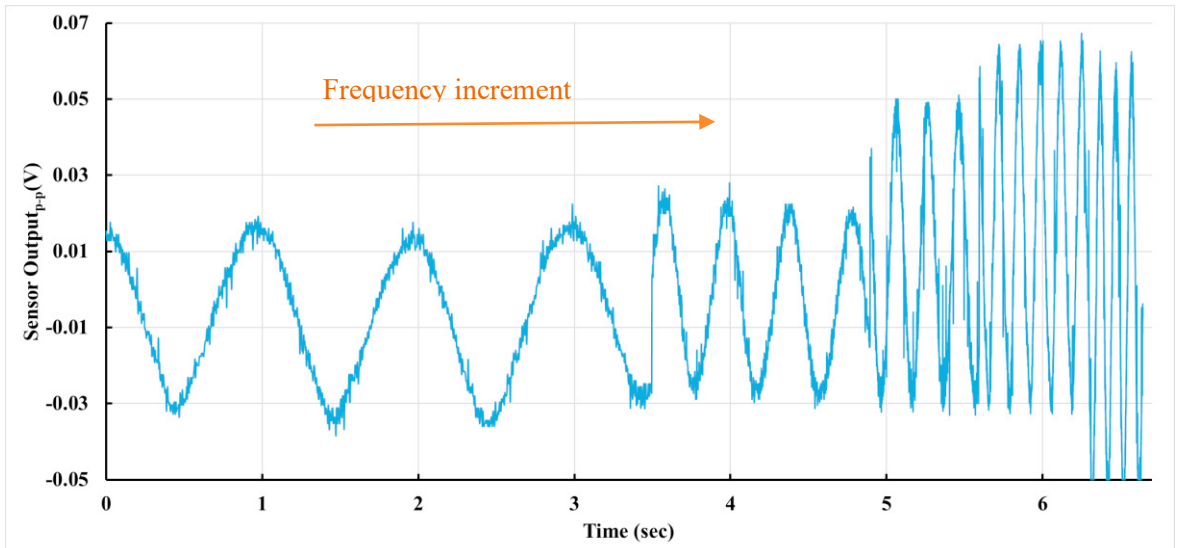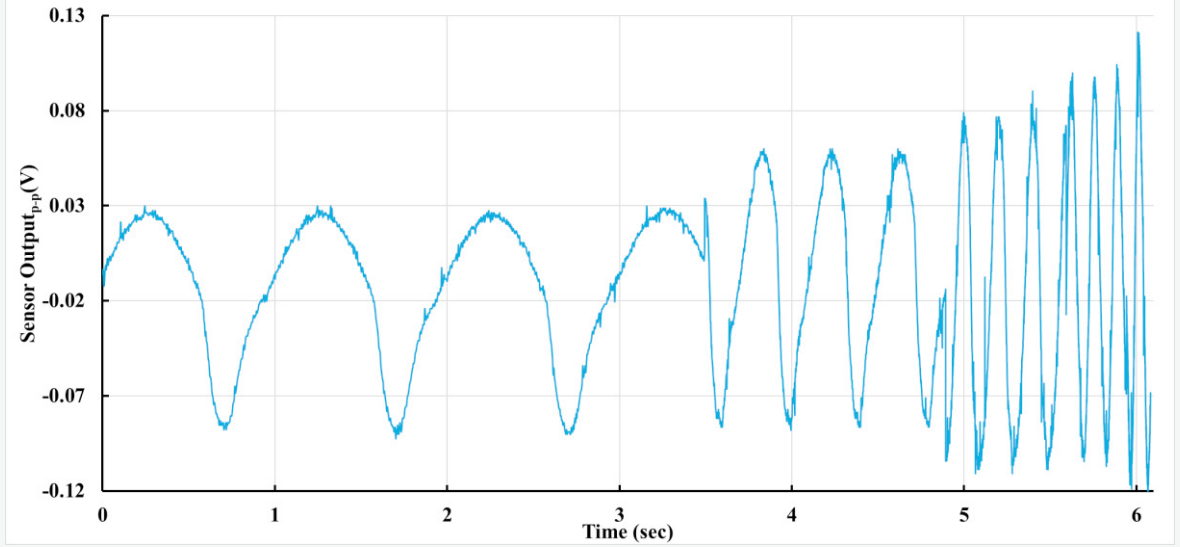

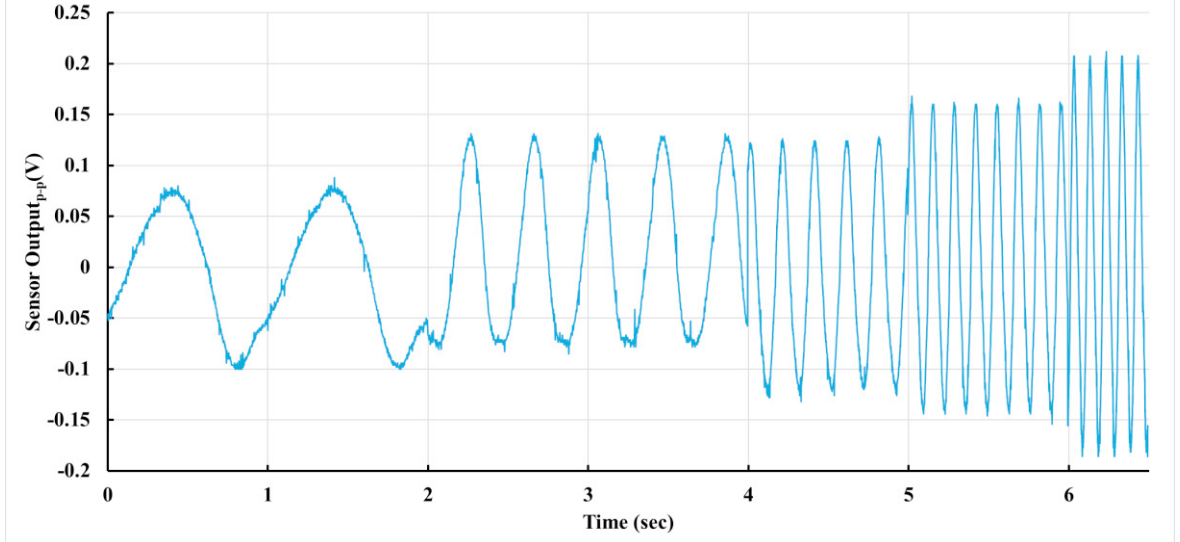Fig. 6. Tension-tension cyclic loading profile
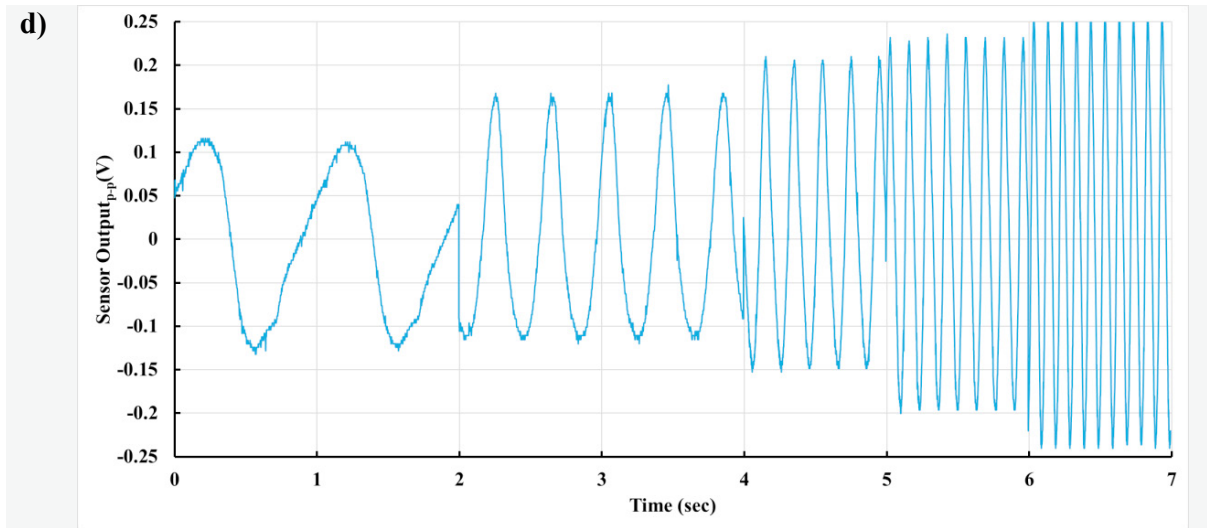
a)

b)

c)

d)

Fig. 7. PZT sensor output in a) 0.2kN to 2kN, b) 0.2kN to 4kN, c) 0.2kN to 6kN, d) 0.2kN to 8kN tension and loading frequency variations
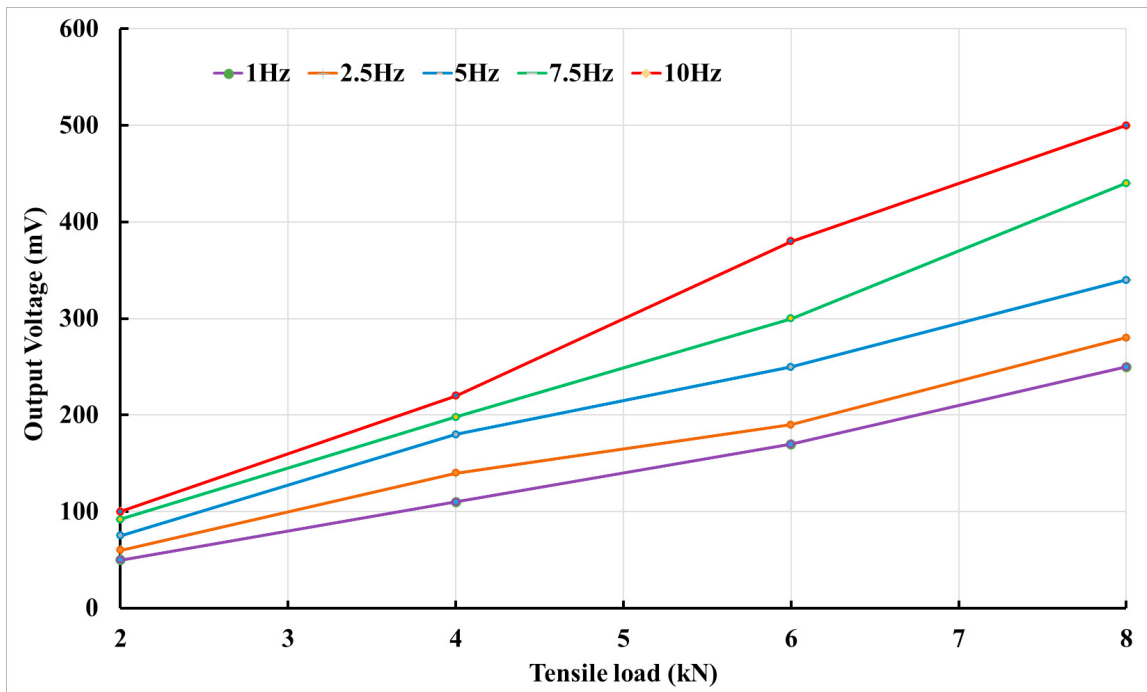

Fig. 8. Output voltage as a function of tensile loading in different loading frequency

5. Conclusions

This research presents a novel extension designed to host PZT sensors for fatigue life monitoring of engineering structures. The extension offers the flexibility of surface-mounting or embedding within the structure, providing a user-friendly interface for strain measurement. By incorporating an initial bending design, the extension mitigates the risk of sensor rupture under high strains. The working principle of the extension allows for the transfer of displacement to the sensor, resulting in the generation of an electrical signal that accurately reflects strain variations in the host structure. The use of the extension simplifies the monitoring process by eliminating the need for different sensor attachments and customized signal analysis for each structure. It was observed that the generated PZT voltage and the strain levels have a linear relationship, with a dependency in the frequency of the cyclic load. Therefore further research is required to understand and explain this frequency dependency in order to make a reliable fatigue life monitoring sensor. In addition, future studies will involve the design of electronic systems for signal conditioning, processing, and communication.

References

[1]   'Structural Health Monitoring (SHM) in Aerospace Structures - Google Books'. https://books.google.nl/books?hl=en&lr=lang_en&id=hrJ0BgAAQBAJ&oi=fnd&pg=PP1&dq=Structur al+health+monitoring+(SHM)+in+aerospace+structures&ots=rTLq2YomY9&sig=K_xUA-m0NG47vXHkZag-kG_VEqw&redir_esc=y#v=onepage&q&f=false (accessed May 27, 2023).

[2]   H. Speckmann and R. Henrich, 'STRUCTURAL HEALTH MONITORING (SHM)-OVERVIEW ON TECHNOLOGIES UNDER DEVELOPMENT'.

[3]   C. R. Farrar and K. Worden, 'An introduction to structural health monitoring', *Philos. Trans. R. Soc. A Math. Phys. Eng. Sci.*, vol. 365, no. 1851, pp. 303–315, Dec. 2006, doi: 10.1098/RSTA.2006.1928.

[4]   A. D. Eslamlou, A. Ghaderiaram, M. Fotouhi, and E. Schlangen, 'A Review on Non-destructive Evaluation of Civil Structures Using Magnetic Sensors', *Lect. Notes Civ. Eng.*, vol. 270 LNCE, pp. 647–656, 2023, doi: 10.1007/978-3-031-07322-9_65/FIGURES/5.

[5]   M. Haq, S. Bhalla, T. N.- Measurement, and undefined 2020, 'Fatigue damage monitoring of reinforced concrete frames using wavelet transform energy of PZT-based admittance signals', *Elsevier*, Accessed: May 27, 2023. [Online]. Available:https://www.sciencedirect.com/science/article/pii/S0263224120305716

[6]   C. Niezrecki, J. Baqersad, A. Sabato, and A. Edu, 'Digital image correlation techniques for non-destructive evaluation and structural health monitoring', *sites.uml.edu*, Accessed: May 27, 2023. [Online]. Available: https://sites.uml.edu/alessandro-sabato/files/2019/09/Niezrecki-er-al.-2019-Digital-image-correlation-techniques-for-NDE-and-SHM.pdf

[7]   K. Čápová, L. Velebil, J. V.- Sensors, and undefined 2020, 'Laboratory and in-situ testing of integrated fbg sensors for shm for concrete and timber structures', *mdpi.com*, 2020, doi: 10.3390/s20061661.

[8]   H. Elahi, M. Eugeni, and P. Gaudenzi, 'Piezoelectric material', *Piezoelectric Aeroelastic Energy Harvest.*, pp. 3–19, 2022, doi: 10.1016/B978-0-12-823968-1.00010-6.

[9]   J. Etxaniz, G. Aranguren, … J. G.-G.-E. F., and undefined 2023, 'Ultrasound-based structural health monitoring methodology employing active and passive techniques', *Elsevier*, Accessed: May 27, 2023. [Online]. Available: https://www.sciencedirect.com/science/article/pii/S1350630723000316

[10]   M. ul Haq, S. Bhalla, T. N.-P. engineering, and undefined 2017, 'Fatigue damage assessment of RC column using PZT sensors', *Elsevier*, Accessed: May 27, 2023. [Online]. Available: https://www.sciencedirect.com/science/article/pii/S1877705816345295

[11]   M. Haq, S. Bhalla, T. N.-C. and C. Composites, and undefined 2020, 'Fatigue damage and residual fatigue life assessment in reinforced concrete frames using PZT-impedance transducers', *Elsevier*, Accessed: May 27, 2023. [Online]. Available: https://www.sciencedirect.com/science/article/pii/S0958946520302778

[12]   S. C. Mukhopadhyay and I. Ihara, 'Sensors and technologies for structural health monitoring: A review', *Lect. Notes Electr. Eng.*, vol. 96, pp. 1–14, 2011, doi: 10.1007/978-3-642-21099-0_1/COVER.

[13]   X. Hu, B. Wang, and H. Ji, 'A Wireless Sensor Network-Based Structural Health Monitoring System for Highway Bridges', *Comput. Civ. Infrastruct. Eng.*, vol. 28, no. 3, pp. 193–209, Mar. 2013, doi: 10.1111/J.1467-8667.2012.00781.X.

[14]   B. P. Nguyen, Q. H. Tran, T. T. Nguyen, A. M. S. Pradhan, and T. C. Huynh, 'Understanding Impedance Response Characteristics of a Piezoelectric-Based Smart Interface Subjected to Functional Degradations', *Complexity*, vol. 2021, 2021, doi: 10.1155/2021/5728679.

[15]   J. Schijve, 'Fatigue of structures and materials', *Fatigue Struct. Mater.*, pp. 1–622, 2009, doi: 10.1007/978-1-4020-6808-9/COVER.

[16]   Y. Luo, H. Zheng, H. Zhang, and Y. Liu, 'Fatigue reliability evaluation of aging prestressed concrete bridge accounting for stochastic traffic loading and resistance degradation', *Adv. Struct. Eng.*, vol. 24, no. 13, pp. 3021–3029, 2021, doi: 10.1177/13694332211017995.

[17]   L. Mei and Q. Wang, 'Structural Optimization in Civil Engineering: A Literature Review', *Buildings*, vol. 11, no. 2, 2021, doi: 10.3390/buildings11020066.

[18]   P. Li, W. Jiang, R. Lu, D. Yuan, J. Shan, and J. Xiao, 'Design and durability of PZT/PVDF composites based on pavement perception', 2022, doi: 10.1016/j.conbuildmat.2022.126621.

[19]   O. Scott-Emuakpor, T. George, C. Cross, and M. H. H. Shen, 'Hysteresis-loop representation for strain energy calculation and fatigue assessment', *J. Strain Anal. Eng. Des.*, vol. 45, no. 4, pp. 275–282, 2010, doi: 10.1243/03093247JSA602.

[20]   Physik Instrumente, 'DuraAct Patch Transducer', no. 10051784, pp. 1–5, 2015.